Quantum Annealing via Environment-Mediated Quantum Diffusion

Vadim N. Smelyanskiy, Davide Venturelli, Alejandro Perdomo-Ortiz, Sergey Knysh, and Mark I. Dykman

Phys. Rev. Lett. **118**, 066802 — Published 10 February 2017

DOI: 10.1103/PhysRevLett.118.066802

Quantum annealing via environment-mediated quantum diffusion

Vadim N. Smelyanskiy,[1,*] Davide Venturelli,[2,3] Alejandro Perdomo-Ortiz,[4,3] Sergey Knysh,[5,3] and Mark I. Dykman[6,†]

[1] *Google, Venice, CA 90291*
[2] *USRA Research Institute for Advanced Computer Science (RIACS), Mountain View CA 94043*
[3] *NASA Ames Research Center, Mail Stop 269-1, Moffett Field CA 94035-1000*
[4] *University of California Santa Cruz, University Affiliated Research Center at NASA Ames*
[5] *Stinger Ghaffarian Technologies Inc., 7701 Greenbelt Rd., Suite 400, Greenbelt, MD 20770*
[6] *Department of Physics and Astronomy, Michigan State University, East Lansing, MI 48824-232*

(Dated: January 13, 2017)

We show that quantum diffusion near a quantum critical point can provide an efficient mechanism of quantum annealing. It is based on the diffusion-mediated recombination of excitations in open systems far from thermal equilibrium. We find that, for an Ising spin chain coupled to a bosonic bath and driven by a monotonically decreasing transverse field, excitation diffusion sharply slows down below the quantum critical region. This leads to spatial correlations and effective freezing of the excitation density. Still, obtaining an approximate solution of an optimization problem via the diffusion-mediated quantum annealing can be faster than via closed-system quantum annealing or Glauber dynamics.

Quantum annealing (QA) has been proposed as a candidate for a speedup of solving hard optimization problems [1–3]. Optimization can be thought of as motion toward the potential minimum in the energy landscape associated with the computational problem. Conventionally, QA is related to quantum tunneling in the landscape that is slowly varied in time [4]. It provides an alternative to simulated annealing, which relies on classical diffusion via thermally activated interwell transitions. It was suggested that the coupling to the environment would not be necessarily detrimental to QA [5–7] .

Recently the role of quantum tunneling as a computational resource has become a matter of active debate [8, 9, 11–13], as it is not necessarily advantageous compared to classical computational techniques, e.g., the path integral Monte Carlo [14–16]. In addition, dissipation and noise can make tunneling incoherent, significantly slowing down [17] the transition rates that underlie QA.

In this paper we show that dissipation-mediated quantum diffusion can provide an efficient additional resource for QA. We model QA as the evolution of a far from thermal equilibrium multi-spin system, which is coupled to a thermal reservoir and is driven by a time-dependent field. The diffusion involves environment-induced transitions between entangled states. These states are delocalized coherent superpositions of multi-spin configurations separated by a large number of spin flips (a large Hamming distance). At a late stage of QA the diffusion coefficient decreases. Ultimately diffusion becomes hopping between localized states and QA is dramatically slowed down. An important question is whether the solution obtained by then is closer to the optimum than the solution obtained over the same time classically.

Diffusion plays a special role where the system is driven through the quantum critical region, as often considered in QA [2, 4, 8]. A well-known result of going through such a region is the generation of excitations via the Kibble-Zurek mechanism [18, 19]. This leads to an error, in terms of QA, as the system is ultimately frozen in the excited state. The generation rate can be even higher in the presence of coupling to the environment [20, 21].

It is diffusion that makes it possible for the excitations to "meet" each other and to recombine, thus reducing their number. Near the critical region diffusion is enhanced because of the large correlation length. It has universal features related to the simple form of the excitation energy spectrum.

The effect of quantum-diffusion induced acceleration of QA is of utmost importance for systems with *delocalized* multi-spin excitations, in particular, above or close to the threshold of many-body localization transition. To reveal and characterize this new effect, we study it here for a model with no disorder. This model is of interest on its own as an example of a far from equilibrium system coupled to the environment. The specific model is a one-dimensional Ising spin chain driven through the quantum phase transition by varying a transverse magnetic field at a constant speed. Among recent applications of this classic model we would mention cold atom systems [23–25] and the circuit QED [26].

We assume that each spin is weakly coupled to its own bosonic bath. The QA Hamiltonian is

$$H_{QA} = -J\sum_{n=1}^{N-1}(\sigma_n^z\sigma_{n+1}^z + g\sigma_n^x) - \sum_{n=1}^{N}\sigma_n^x X_n + H_B, \quad (1)$$

where N is the number of spins, $Jg(t)$ is the transverse field, σ_n^x, σ_n^z are Pauli matrices, $H_B = \sum_{n,\gamma}\hbar\omega_{\gamma n}b_{\gamma n}^\dagger b_{\gamma n}$ is the baths Hamiltonian; $X_n = \sum_\gamma \lambda_{\gamma n}(b_{\gamma n}^\dagger + b_{\gamma n})$, and $b_{\gamma n}^\dagger, b_{\gamma n}$ are boson creation/annihilation operators in the nth bath. We assume Ohmic dissipation,

$2\sum_\gamma(\lambda_{\gamma n}/\hbar)^2\delta(\omega-\omega_{\gamma n})=\alpha\omega$, $\alpha\ll 1$, and linear in time schedule for reducing the transverse field, $\dot g(t)=-v<0$, starting from the initial value $g_i\gg 1$. We further assume translational symmetry, so that $\lambda_{\gamma n},\omega_{\gamma n}$ are independent of n. The spin-boson coupling (1) provides a microscopic model for the classical spin-flip process in the Glauber dynamics [27].

In the absence of coupling to the environment, model (1) describes a quantum phase transition between a paramagnetic phase ($g>1$) and a ferromagnetic phase ($g<1$) [28]. The spin part of the Hamiltonian (1) can be mapped onto fermions [29] using the Jordan-Wigner transformation, $\sigma_n^x=1-2a_n^\dagger a_n$, $\sigma_n^z=-K(n)(a_n^\dagger+a_n)$ where $K(j)=\prod_{i<j}\sigma_i^x$; $a_n^\dagger$ and a_n are fermion creation and annihilation operators. Changing in the standard way to new creation and annihilation operators $\eta_k^\dagger$, η_k, with $\eta_k=\frac{1}{\sqrt{N}}\sum_{n=1}^N[a_n\cos(\theta_k/2)-ia_n^\dagger\sin(\theta_k/2)]e^{-ikn}$, we obtain the Hamiltonian of the isolated spin chain as $H_0=2J\sum_k\epsilon_k\eta_k^\dagger\eta_k$, where ϵ_k is the dimensionless fermion energy,

$$\epsilon_k=\sqrt{(g-\cos k)^2+\sin^2 k},\quad \tan\theta_k=\frac{\sin k}{g-\cos k}. \tag{2}$$

The dependence of the minimal energy $\Delta=2J\epsilon_0$ on g and the form of ϵ_k are illustrated in Fig. 1.

In the course of QA, pairs of fermions with opposite momenta are born from vacuum due to the Landau-Zener transitions as the system passes through the critical point $g=1$ [18, 19]. The resulting density of excitations $n_{\rm KZ}$ for large N is simply related to the QA speed [31],

$$n_{\rm KZ}=|\hbar\dot g/8\pi J|^{1/2}. \tag{3}$$

In terms of the fermion operators, the Hamiltonian of the coupling to bosons, Eq. (1), reads

$$H_i=\sum_{kk'}h_{kk'}X_{k-k'},$$
$$h_{kk'}=c_{kk'}\eta_k^\dagger\eta_{k'}+s_{kk'}\eta_k^\dagger\eta_{-k'}^\dagger+s_{k'k}^*\eta_{-k}\eta_{k'}, \tag{4}$$

where $X_q=\sum_\gamma\lambda_\gamma(b_{\gamma q}+b_{\gamma\,-q}^\dagger)$ are boson field operators, $b_{\gamma q}=N^{-1/2}\sum_n b_{\gamma n}\exp(-iqn)$; the coefficients $c_{kk'}$ and $s_{kk'}$ are expressed in terms of the rotation angles θ_k,θ_q, see Eq. (24) of the Supplemental Material (SM) [32].

From Eq. (4) one can identify three types of relaxation processes, see Fig. 1(b,c). The first is scattering by a boson in which a fermion changes its momentum k and energy ϵ_k. The rate of a single-fermion transition $k\to k'$ is $W_{kk'}^{+-}\propto|c_{kk'}|^2$. The other processes are generation and recombination of pairs of fermions due to boson scattering. The parity of the total number of fermions is not changed. The generation and recombination rates $W_{kk'}^{++}$ and $W_{kk'}^{--}$ are $\propto|s_{kk'}|^2$,

$$W_{kk'}^{\mu\nu}=\frac{2\pi\alpha}{N}\Omega_{kk'}^{\mu\nu}\left[1-\mu\nu\cos(\mu\theta_k-\nu\theta_{k'})\right]\left[\bar n(\Omega_{kk'}^{\mu\nu})+1\right],$$
$$\Omega_{kk'}^{\mu\nu}=2J(\mu\epsilon_k+\nu\epsilon_{k'})/\hbar, \tag{5}$$

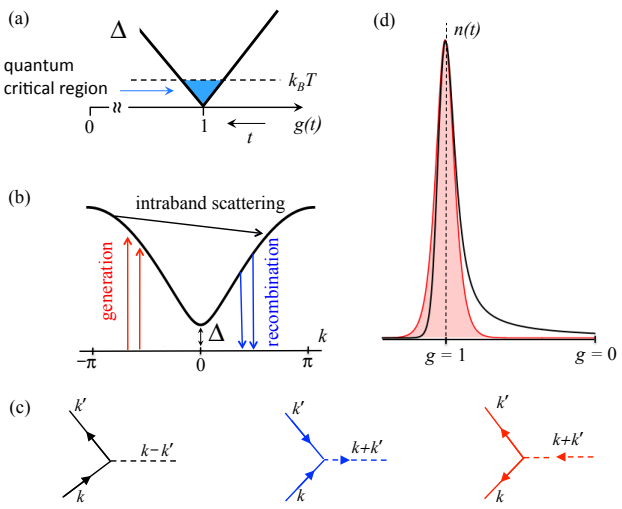

Figure 1. (a) The dependence of the gap Δ in the energy spectrum of the Ising chain (2) on the scaled transverse field g, which linearly decreases in time. (b) The fermion dispersion law and the processes of fermion scattering induced by the coupling to the Bosonic field. Both the generation and the recombination are two-fermion processes. (c) The diagrams that show single-fermion intraband scattering, recombination, and generation of fermions; the change of the fermion energy and momentum comes from the bosons. (d) The dependence of the density of quasiparticles on time ($g=1-\dot gt$). The boundary of the filled region shows the thermal equilibrium density, whereas the solid line shows the nonequilibrium density calculated using the Boltzmann equation (6) and disregarding spatial correlations.

where $\mu,\nu=\pm$ and $\bar n(\omega)=[\exp(\hbar\omega/k_BT)-1]^{-1}$.

The single-particle quantum kinetic equation that incorporated these processes was considered in Ref. [20, 21]. It was written for the coupled fermion populations $\langle\eta_k^\dagger\eta_k\rangle$ and coherences $\langle\eta_k\eta_{-k}\rangle$. The approach [20, 21] involved two major approximations, the spatial uniformity of the fermion distribution and the absence of fermion correlations. These approximations hold in the critical region, where the gap in the energy spectrum $\Delta(g)=2J|1-g|\lesssim k_BT$. For a sufficiently low QA rate, the density of excitations is dominated by thermal processes rather than the Landau-Zener tunneling [20, 21]. The fermion population in this region is $[\exp(2J\epsilon_k/k_BT)+1]^{-1}$, see Fig. 1(d).

QA aims at minimizing the number of excitations over a given time. As we show, for the considered open system there exists an optimal QA speed that allows one to achieve the excitation density far below the Landau-Zener-limited density (3) in a closed system. This density corresponds to the bottleneck of QA imposed by the sharp slowing down of excitation decay due to many-fermion effects and spatial correlations. The approximation [20, 21] does not capture this effect. The full analysis requires solving the full Bogolyubov chain of equations for the coupled many-particle Green's functions [22]. However, the density where the slowing down

occurs and the scaling relations between the speed $\dot{g}$ and the final density of excitations, which are our primary interest, can be found in a simpler way, as discussed below.

As we show, of interest is the range of g behind the critical region, yet close to it, where $1-g \ll 1$. In this range, as g decreases, spatial correlations in the fermion system change from weak to strong. We start with the region of comparatively high densities, where spatial correlations can be disregarded and the fermion dynamics is described [30] by the Boltzmann equation for the *single-fermion* Wigner probability density $\rho_W(x,k) = (2\pi)^{-1}\int dp \langle \eta^\dagger_{k+p/2}\eta_{k-p/2}\rangle e^{-ipx}$,

$$\partial_t \rho_W + \frac{2J}{\hbar}(\partial_k \epsilon_k)\partial_x \rho_W = \hat{\mathcal{L}}^{(0)}[\rho_W] + \hat{\mathcal{L}}^{(1)}[\rho_W]. \quad (6)$$

Here, operator $\hat{\mathcal{L}}^{(0)}$ describes single-fermion scattering by bosons [30], see Fig. 1, with the transition rates $W^{+-}_{kk'}$ given by Eq. (5), cf. Eqs. (6) and (9) in SM. The characteristic reciprocal relaxation time of fermion momentum due to single-fermion scattering τ_r^{-1} is determined by the transition rate $W^{+-}_{kk'}$ for fermions with energies $2J\epsilon_k, 2J\epsilon_{k'} \sim k_BT$,

$$\tau_r^{-1}(g) = 2\alpha k_B T[(1-g)/\beta g\hbar^2]^{1/2}, \quad \beta = 2J/k_BT. \quad (7)$$

This expression refers to the semiclassical range behind the critical point where the excitation gap Δ has become large compared to k_BT,

$$e^{-\Delta(g)/k_BT} \ll 1, \quad \Delta(g) = 2J(1-g). \quad (8)$$

The rate $\tau_r^{-1}(g)$ increases with the distance $1-g \propto \Delta$ from the critical point. Extrapolating it back to the critical region $\Delta \simeq k_BT$, we recover the scaling of the critical relaxation rate $(\tau_r^{-1})_{\rm c}$ found in [20, 21]. For slow quantum annealing rate that we consider,

$$J|\dot{g}| \ll \hbar(\tau_r^{-1})_{\rm c}, \qquad (\tau_r^{-1})_{\rm c} \simeq 4J\alpha/\hbar\beta^2, \quad (9)$$

the fermion distribution in the critical region remains of the Boltzmann form.

Operator $\hat{\mathcal{L}}^{(1)}[\rho_W]$ in Eq. (6) describes two-fermion generation and recombination accompanied, respectively, by absorption and emission of a boson, see Fig. 1. Recombination requires a collision of two fermions with a boson, see Fig. 1. Respectively, the recombination term is quadratic in ρ_W,

$$\hat{\mathcal{L}}^{(1)}_{\rm rec}[\rho_W(x,k)] = -N\sum_q W^{++}_{kq}\rho_W(x,k)\rho_W(x,q). \quad (10)$$

It becomes small for small fermion densities. In contrast, the generation term $\hat{\mathcal{L}}^{(1)}_{\rm gen}[\rho_W(x,k)]$ is density-independent for small densities and is proportional to $W^{--}_{kq} \propto \exp[-\Delta(g)/k_BT]$. It rapidly falls off as the control parameter g moves away from the critical point.

Overall, in the range (8) the generation and recombination rates described by $\hat{\mathcal{L}}^{(1)}$ are small compared to the momentum relaxation rate τ_r^{-1}, and the distribution over the fermion momentum approaches thermal equilibrium with the bosonic bath temperature. Function $\rho_W(x,k)$ in (6) factors into a product of the Boltzmann distribution over fermion energy ϵ_k and a coordinate-dependent fermion density $n(x,t)$, $\rho_W = n(x,t)\exp(-\beta\epsilon_k)/\sum_k \exp(-\beta\epsilon_k)$.

A new time scale is associated with the decay of density fluctuations. In the considered approximation this decay is described by the diffusion equation

$$\dot{n}(x,t) = D\partial_x^2 n(x,t), \quad D = c_D\frac{J\beta^{1/2}}{\alpha\hbar}\frac{g^{3/2}}{(1-g)^{3/2}}. \quad (11)$$

The diffusion coefficient (11) has a standard form $D \sim \langle v_k^2\rangle\tau_r$ with $v_k = (2J/\hbar)\partial_k\epsilon_k$ being the fermion velocity; D sharply increases with decreasing $1-g$. In Eq. (11) $c_D \approx 0.17$ [32].

On the time long compared to the decay time of density fluctuations, the distribution $n(x,t)$ becomes uniform and its evolution is determined by generation and recombination processes. The spatially-averaged density $\langle n\rangle$ is described by a rate equation,

$$\langle \dot{n}\rangle = -w(\langle n\rangle^2 - n_{\rm th}^2). \quad (12)$$

Here, $n_{\rm th} \equiv n_{\rm th}(g) = N^{-1}\sum_k \exp(-\beta\epsilon_k)$ is the thermal equilibrium density, whereas $w(g) = \sum_{k,q} W^{++}_{kq}\exp[-\beta(\epsilon_k+\epsilon_q)]/Nn_{\rm th}^2$ is the recombination rate. From Eq. (5), for $\beta \gg 1-g, 1/g$

$$w(g) \simeq \frac{8\pi\alpha J}{\hbar\beta g}, \quad n_{\rm th}(g) \simeq \left(\frac{1-g}{2\pi\beta g}\right)^{1/2} e^{-\beta(1-g)}. \quad (13)$$

As $g \equiv g(t)$ decreases, the thermal density $n_{\rm th}$ exponentially sharply falls down. The mean density $\langle n\rangle$ cannot follow this decrease, so that the density of fermions becomes higher than the thermal density. This happens for the value $g(t) = g_{\rm th}$ where the correction $\delta\langle n\rangle = \langle n(t)\rangle - n_{\rm th}\big(g(t)\big)$ becomes $\sim n_{\rm th}\big(g(t)\big)$, see Figs. 1 and 2. The quasistationary solution of the linearized Eq. (12) reads $\delta\langle n\rangle \approx -\dot{n}_{\rm th}/2wn_{\rm th}$. This gives an equation for $g_{\rm th}$

$$\beta^{-1}w(g)n_{\rm th}(g) = |\dot{g}| \quad \text{for} \quad g = g_{\rm th}. \quad (14)$$

As g is decreased below $g_{\rm th}$ and reaches the region $\exp\{\beta[g_{\rm th} - g(t)]\} \gg 1$, we can disregard $n_{\rm th}$ in Eq. (12). Then using the explicit form of the rate $w(g)$, we obtain

$$\langle n(t)\rangle \approx \beta^{-1}n_{\rm th}(g_{\rm th})\Big(\log\left[g_{\rm th}/g(t)\right]\Big)^{-1}. \quad (15)$$

This expression describes quantum annealing of fermion density in a strongly nonequilibrium regime. We observe that $\langle n(t)\rangle$ varies with time only logarithmically here.

For still smaller g, not only the system moves further away from thermal equilibrium in terms of $\langle n\rangle$, but it also develops strong spatial fluctuations. This

is due to the sharp decrease of the diffusion coefficient $D = D(g)$, see Eq. (11). Spatial fluctuations of the density $n(x,t)$ impose a bottleneck on the recombination in one-dimensional systems [38], because for fermions to recombine they first have to come close to each other. In contrast to the usually studied reaction-diffusion systems, in the present case the bottleneck arises not because of the decrease of the density, but, in the first place, because of the falloff of the diffusion coefficient. Once the recombination becomes limited by diffusion, the change of the fermion density becomes slower than in Eq. (15).

To estimate the density $n_* = \langle n(t_*)\rangle$ where the crossover to diffusion-limited recombination occurs we set the rates $\dot{n}$ of the recombination and diffusion processes equal to each other. For the recombination, one can use Eq. (12), $\dot{n} = -wn^2$. For the diffusion, one can use Eq. (11) where the mean inter-particle distance $1/\langle n\rangle$ is chosen as a spatial scale on which the density fluctuates. This gives

$$n_* = \langle n(t_*)\rangle = kw(g_*))/D(g_*), \qquad g_* = g(t_*), \quad (16)$$

where $k \sim 1$. An alternative way of estimating n_* is described in Sec. IV of the SM.

Equations (14) - (16) relate the crossover value of $g = g_*$ to the value $g_{\rm th}$ where thermal equilibrium is broken. Since $g_*, g_{\rm th}$ are close to the critical point $g = 1$, it is convenient to switch to variable $z = \beta(1-g)$, with $z_* = \beta(1-g_*)$ expressed in terms of $z_{\rm th} = \beta(1-g_{\rm th})$ as follows:

$$\mu(\beta/\alpha)^2 z_{\rm th}^{1/2}\exp(-z_{\rm th}) = z_*^{3/2}(z_* - z_{\rm th}), \quad (17)$$

where $\mu = c_D/8k\sqrt{2\pi^3}$; note that $\beta/\alpha \gg 1$. Equations (14) - (17) express the crossover density n_* in terms of the speed $|\dot{g}|$.

Beyond the crossover point, $g < g_*$ (i.e., $t > t_*$), the diffusion-controlled decrease with time of the already small fermion density is further significantly slowed down compared to Eq. (15). If we stop QA once g_* is reached, n_* gives the approximate solution of the annealing problem. Unexpectedly, the dependence of n_* and g_* on $|\dot{g}|$ is nonmonotonic, see Fig. 2. The optimal (minimal with respect to $|\dot{g}|$) value of n_* is

$$n_{\rm opt} \approx [8\pi k\alpha^2/c_D\beta^3]z_{\rm opt}^{3/2}, \quad (18)$$

where $z_{\rm opt} \equiv \beta(1-g_{\rm opt}) \approx \log[\mu(\beta/\alpha)^2]$ is the value of z_* where n_* is optimal. The optimal speed is

$$|\dot{g}|_{\rm opt} \approx (64k\pi^2 J\alpha^3/c_D\beta^5\hbar)\ln(\beta^2/\alpha^2)^{1/2}. \quad (19)$$

Equation (9) suggests that, in the considered dissipative system, QA can be started at the critical point. Then the time $z_{\rm opt}/\beta|\dot{g}|_{\rm opt}$ to reach $g_{\rm opt}$ is a small portion of the total time to reach $g = 0$, which is $|\dot{g}|_{\rm opt}^{-1}$. The density $n_{\rm opt}$ is extremely small for weak coupling, $\alpha \ll 1$, and low temperatures, $\beta \gg 1$, and it rapidly decreases with decreasing α and k_BT/J.

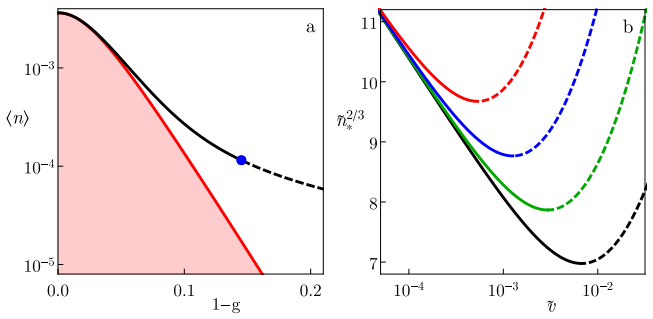

Figure 2. Fermion density vs. the distance to the critical point (a) and vs. the annealing rate (b). In (a), the filled region is bound by the thermal distribution $n_{\rm th}(g)$. The black line shows the nonequilibrium density $\langle n\rangle$ for $\alpha = 0.06$, $\beta = 25$ and $|\dot{g}|$=$|\dot{g}|_{\rm opt}$=2.85 $\times$ 10^{-7}, see Eq. (12). The blue point marks the crossover value g_*. For $g < g_*$ spatial correlations become strong and the theory is inapplicable. In (b), the red, blue, green and black lines show the scaled density $\tilde{n}_* = c_d\beta^3 n_*/8k\pi\alpha^2$ vs. the scaled QA rate $v = \hbar\beta^3|\dot{g}|/4\sqrt{2\pi}J\alpha$ for $\log\mu = 8, 9, 10, 11$, respectively [parameter $\mu \propto (\beta/\alpha)^2$ is defined in (17)]. The minimal density $n_{\rm opt} = \min n_*$. The dashed sections of the lines refer to the regions where the asymptotic theory does not apply.

The evolution of the fermion density for $t > t_*$ can be roughly estimated from the scaling equation $\langle\dot{n}\rangle = -k'D(g)\langle n\rangle^3$, cf. [38], where $k' \sim 1$. Because of the sharp decrease of $D(g)$ with increasing $1-g$, the solution of this equation for $1 - g = \mathcal{O}(1)$ weakly depends on $g(t)$. For the optimal speed (19) such saturation density is $\langle n\rangle \sim n_{\rm opt}/\ln(\beta/\alpha) \ll n_{\rm opt}$.

It is instructive to compare the optimal speed (19) with the speed $|\dot{g}|_{\rm KZ}$ that would lead to the same saturation density $n_{\rm opt}/\ln(\beta/\alpha) = n_{\rm KZ}$ due to the Kibble-Zurek mechanism of the creation of excitations in the absence of coupling to the environment. From Eqs. (3) and (19),

$$\dot{g}_{\rm opt}/\dot{g}_{\rm KZ} \propto (\beta/\alpha)\ln(\beta/\alpha)^2 \gg 1. \quad (20)$$

Therefore the time it takes to reach the approximate solution (18) in a closed quantum system is much larger than in our case.

It is instructive also to compare $|\dot{g}|_{\rm opt}$ with the speed of annealing based on the classical Glauber dynamics [27]. In this dynamics, for $k_BT \ll J$ excitations in the Ising spin chain are eliminated through diffusion of kinks. If the transition rate for a kink to move to a neighboring site is $w_{\rm G}$ and the initial density of the kinks is ~ 1, the time $t_{\rm class}$ to reach density $n \ll 1$ is $(8\pi w_{\rm G}n^2)^{-1}$ [27]. In terms of our model, the uncertainty relation imposes a limitation $w_{\rm G} \ll J/\hbar$. Therefore the ratio of the times to reach $n_{\rm opt}/\ln(\beta/\alpha)$ via classical and quantum diffusion is very large, $\sim t_{\rm class}|\dot{g}|_{\rm opt} \propto \beta/\alpha \gg 1$.

The results demonstrate that quantum diffusion near the critical point provides an important mechanism of the speedup of QA. The diffusion occurs over states that are

large quantum superpositions of spin configurations separated by the Hamming distance $\sim \beta g[\alpha(1-g)]^{-1} \gg 1$ of the order of the mean free path of a fermion. The bottleneck of QA in an open system can be imposed by the sharp slowing down of the diffusion behind the critical region. The crossover to slow excitation recombination is accompanied by the onset of significant spatial fluctuations of the excitation density even in the absence of disorder. At the crossover, the residual density of excitations non-monotonically depend on the quantum annealing rate $|\dot{g}|$. Its minimum provides the optimal value of the rate. This value scales with the coupling constant and temperature as $\alpha^3 T^5$, the optimal excitation density is $\propto \alpha^2 T^3$. Importantly, the optimal speed $|\dot{g}|_{\rm opt}$ is independent of the system size.

For our simple but nontrivial example of QA, attaining the approximate solution [40] via the quantum-diffusion mediated process is faster than via classical diffusion or the closed-system QA. One might expect that, in higher-dimensional systems, quantum diffusion over extended states could provide an efficient route to finding approximate solutions in the presence of disorder above the many-body mobility edge [41].

This work was supported in part by the Office of the Director of National Intelligence (ODNI), Intelligence Advanced Research Projects Activity (IARPA), via IAA 145483, by the AFRL Information Directorate under grant F4HBKC4162G001, and by NASA (Sponsor Award Number NNX12AK33A). D.V. and A.P.-O. were also supported in part by Sandia National Laboratory AQUARIUS project. M.I.D. is grateful to the NASA Ames Research Center for the warm hospitality and partial support during his sabbatical.

* smelyan@google.com
† dykman@pa.msu.edu

[1] T. Kadowaki and H. Nishimori, Phys. Rev. E 58, 5355 (1998).
[2] J. Brooke, et al, Science **284**, 779 (1999).
[3] E. Farhi, at el., Science **292**, 472 (2001).
[4] A. Das and B. K. Chakrabarti, Lect. Notes Phys. 679 (Springer, Berlin 2005).
[5] M. H. S. Amin, C. J. S. Truncik, and D. V. Averin, Phys. Rev. A **80**, 022303 (2009).
[6] M. W. Johnson, et al., Nature **473**, 194 (2011).
[7] N. G. Dickson *et al.* Nat. Comm. **4**, 1903 (2013).
[8] G. E. Santoro, et al., Science **295**, 2427 (2002).
[9] S. Morita and H. Nishimori, J. Math. Phys. **49**, 125210 (2008).
[10] J. A. Smolin and G. Smith, Front. Phys. **2**, 52 (2014).
[11] E. Crosson, and A. W. Harrow, IEEE 57th Annual Symposium on Foundations of Computer Science, 714 (2016).
[12] M. B. Hastings, Quant. Info. Comp. **13**, 1038 (2013).
[13] B. Heim *et al.*, Science **348**, 215 (2015).
[14] S. V. Isakov *et al.*, Phys. Rev. Lett. **117**, 180402 (2016).
[15] S. Muthukrishnan, T. Albash, and D. A. Lidar, Phys. Rev. X **6**, 031010 (2016).
[16] S. Mandra, Z. Zhu, W. Wang, et al., Phys. Rev. A **94**, 022337 (2016).
[17] "Quantum Tunneling in Condensed Media", Eds. Y. Kagan and A. J. Leggett (North-Holland, Amsterdam 1992).
[18] T. W. B. Kibble, J. Phys. A **9**, 1387 (1976)
[19] W. H. Zurek, Nature **317**, 505 (1985).
[20] D. Patanè *et al.*, Phys. Rev. Lett. **101**, 175701 (2008).
[21] D. Patanè *et al.*, Phys. Rev **B 80**, 024302 (2009).
[22] G. Stefanucci and R. van Leeuwen, "Nonequilibrium Many Body Theory of Quantum Systems" (CUP, Cambridge, 2013)
[23] P. P. Orth, I. Stanic, and K. L. Hur, Phys. Rev. A **77**, 051601(R) (2008).
[24] H. Schwager, J. I. Cirac, and G. Giedke, Phys. Rev. A **87**, 022110 (2013).
[25] A. W. Carr, M. Saffman, Phys. Rev. Lett. **111**, 033607 (2013).
[26] O. Viehmann, J. von Delft, and F. Marquardt, Phys. Rev. Lett. **110**, , 030601 (2013).
[27] R. Glauber, J. Math. Phys. **4**, 294 (1961).
[28] S. Sachdev, Quantum Phase Transitions, (CUP, Cambridge 1999).
[29] E. Lieb, T. Schultz, and D. Mattis, Ann. Phys. (N.Y.) **16**, 407 (1961).
[30] A Altland and B. Simons, Condensed Matter Field theory (CUP, Cambridge 2010)
[31] J. Dziarmaga, Phys. Rev. Lett. **95**, 245701 (2005).
[32] See Supplemental Material [url], which includes Refs. [33-39].
[33] A. O. Caldeira and A. J. Leggett, Ann. Phys. (N.Y.) **149**, 374 (1983).
[34] D. Ben Avraham, M. Burschka, and C. Doering, J. Stat. Phys. **60**, 695 (1990).
[35] V. Privman, C. R. Doering, and H. L. Frisch, Phys. Rev. E **48**, 846 (1993)
[36] D. C. Mattis and M. L. Glasser, Rev. Mod. Phys. **70**, 979 (1998).
[37] J. Allam et al., Phys. Rev. Lett. **111**, 197401 (2013).
[38] Uwe C. Tauber, Critical Dynamics: A Field Theory Approach to Equilibrium and Non-Equilibrium Scaling Behavior (Cambridge University Press, Cambridge 2014).
[39] M. Smoluchowsky, Z. Phys. Chem. **92**, 129 (1917).
[40] E. Farhi, J. Goldstone, S. Gutmann, arXiv:1411.4028 [quant-ph].
[41] C. R. Laumann, A. Pal, and A. Scardicchio, Phys. Rev. Lett. **111**, 200405 (2014).